Genetic-Algorithm-Based Parameter Estimation Technique for Fragmenting Radar Meteor Head Echoes

Arnab Roy, Stan J. Briczinski, John F. Doherty, *Senior Member, IEEE*, and John D. Mathews, *Senior Member, IEEE*

***Abstract*—Meteoroid fragmentation presents a serious problem for Doppler estimation using Fourier transform techniques. Radar returns from multiple closely spaced bodies traveling at nearly identical speeds result in an interference pattern which makes it difficult to estimate properties of individual bodies by traditional techniques. Here, we present a genetic-algorithm-based procedure to determine the properties of the individual fragments, such as relative scattering cross section, speed, and deceleration. The radar meteor observations presented here were made using the Poker Flat (Alaska) Incoherent Scatter Radar operating at 449.3 MHz.**

***Index Terms*—Fragmentation, genetic algorithms (GAs), meteor head echoes, parameter estimation.**

I. Introduction

THE SCIENTIFIC community has been interested in observing sporadic radar meteors due to the role of meteoroids in understanding space weather, in the aeronomy of the meteor zone, and in various aspects of plasma physics [1], [2]. Here, we consider head-echo observations in which radar returns are from the distribution of plasma immediately surrounding the meteoroid and that travels with the meteoroid itself. For details regarding scattering mechanism and models of head echoes, the reader is referred to [1], [3]–[5]. For meteor events observed in more than four radar pulses, a fast-Fourier-transform (FFT)-based technique has been developed that provides estimates of the event altitude, signal-to-noise ratio (SNR), and speed as a function of time throughout the event [6]–[9]. Many events having high enough SNR also yield deceleration estimates.

Fragmented meteoroids present a problem for speed estimation using FFT techniques. Scattering from two nearby slowly separating point targets (relative to the wavelength) exhibits strong interference effects as the two signals add in phase and out of phase. That is, two (or more) common-trajectory meteoroid fragments exist within the radar range resolution cell, and as the scattered electric fields exhibit nearly common Doppler phase effects, the net electric field at the receiver shows a strong interference pattern. Some researchers have previously tried to estimate the properties of fragmented meteoroids [10], [11]. Furthermore, Close *et al.* [12] reported evidence of fragmentation based on their observations but stopped short of analyzing them. We present here a genetic-algorithm (GA)-based [13], [14] optimization technique that searches the multidimensional fragment parameter space to find the parameter set that minimizes some cost function. We use the mean squared error (MSE) between the actual and the estimated signals as the cost function in our study. The radar meteor data used in this study were obtained using the high-power large-aperture radar located at Poker Flat, AK. The Poker Flat Incoherent Scatter Radar (PFISR) was employed in the 96-panel manifestation for these observations. Operational parameters in this mode include 1-MHz sampling rate, 90-μs pulse length, and interpulse period (IPP) of 2 ms.

The characteristics of the fragmented meteoroids such as relative scattering cross section, speeds, and decelerations (relative masses) are estimated using a two-step procedure. In the first step, the radial speed and deceleration of the system of meteoroid fragments are estimated from the Doppler frequency shift in consecutive radar return pulses using FFTs. The initial speed and deceleration estimates from the first step define the parameter search space for the second stage which is a GA-based signal parameter estimator. The GA-based algorithm seeks to find the parameters within the search space that minimizes the MSE between the actual signal and the signal synthesized using the chosen parameters. The ability of this technique to estimate the parameters of a two-fragment system was verified using synthetic radar meteor signals. Then, we applied this technique to PFISR data. Details about this technique and results from our study are presented in the following sections.

II. Coarse Parameter Estimation of Meteoroid Fragments

We focus on three events exhibiting interference patterns recorded by the PFISR. Event 1 [corresponding to Fig. 1(a)] is used to illustrate the technique, while only the final estimated parameters for events 2 and 3 (corresponding to Fig. 1(b) and (c), respectively) are presented here. Before application of the two-step parameter estimation technique, we need to preprocess the data. This involves removing the effect of antenna gain pattern from the data. This step is performed by passing the data through a low-pass filter which produces an estimate of the antenna gain pattern, and the data are then processed using

Manuscript received June 14, 2008; revised August 27, 2008 and December 4, 2008. First published March 4, 2009; current version published July 4, 2009. This work was supported by the National Science Foundation under Grant ITR/AP 04-27029.

A. Roy, J. F. Doherty, and J. D. Mathews are with the Communications and Space Sciences Laboratory, The Pennsylvania State University, University Park, PA 16802-2707 USA.

S. J. Briczinski is with the Department of Physics, University of Wisconsin, Madison, WI 53706 USA.

Digital Object Identifier 10.1109/LGRS.2009.2013878

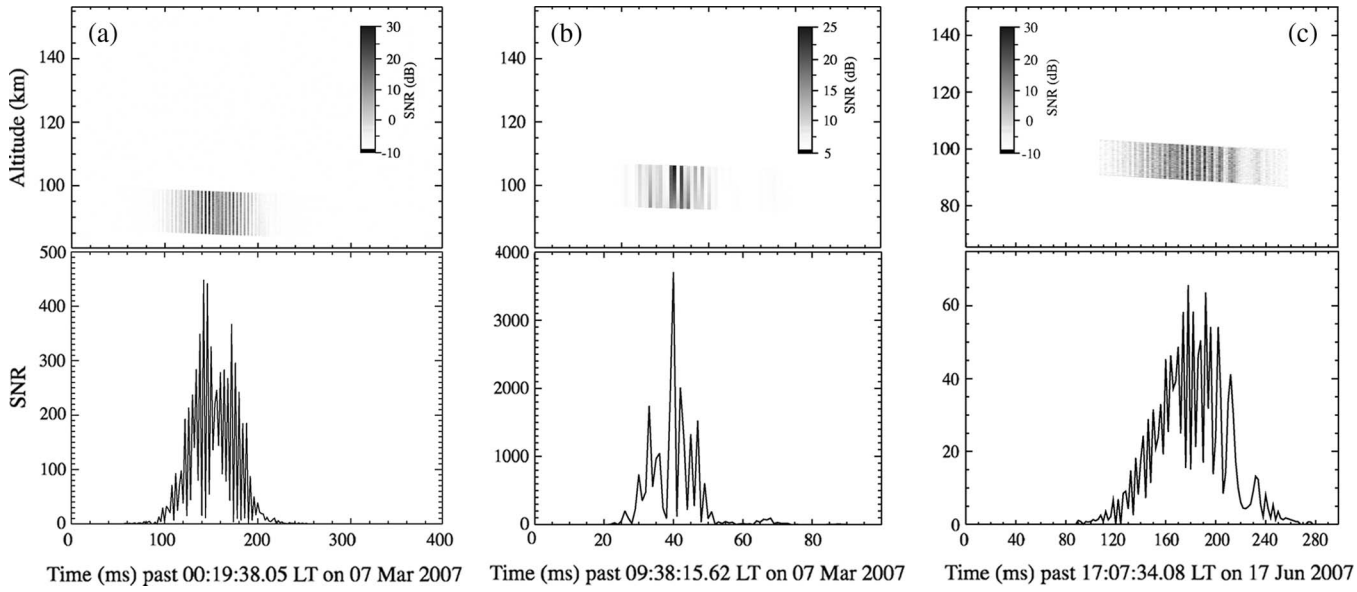

Fig. 1. RTI and SNR (similar to optical meteor light curves) of three meteor events observed with the 449.3-MHz PFISR. The (a) event (Event 1) is consistent with two meteoroids traveling along the same trajectory and each producing a head echo that resulted in the strong interference pattern. The (b) event (Event 2) shows a more complex structure that is consistent with three meteoroid fragments. The (c) event (Event 3) which shows strong frequency modulation of the SNR curve is otherwise similar to event 1.

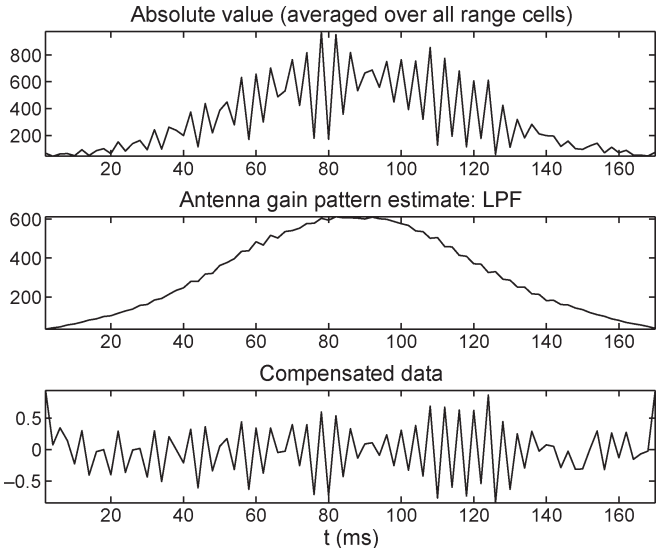

Fig. 2. Event 1 power signal at various stages of the preprocessing step to estimate and remove antenna pattern.

this estimate to compensate for the varying antenna gains for different IPPs. The results of this procedure applied to event 1 are shown in Fig. 2. Furthermore, it is observed that the IPPs at the two extremes of the event have low SNR and are thus ignored for further processing. We only consider 50 central IPPs out of 85 present in event 1.

Next, we form an initial estimate of the Doppler speed and deceleration of the meteoroid fragments by examining the FFT of the data. The Doppler speed is determined using the method described in [7]: the FFT is evaluated for each radar pulse, and the location of the peak absolute value gives the dominant frequency component present in the pulse. It is found that the individual Doppler estimates vary substantially for each IPP. This variation is due in part to the large variations in SNR for each IPP due to fading. However, even in most of the deep nulls, the SNR remains substantial. Another source of Doppler error is that the phase evolution during each pulse is somewhat ambiguous due to the presence of two similar Doppler signatures. A general decrease in the estimated speed as time progresses is also observed that indicates deceleration. The deceleration can be estimated from the slope of the linear fit to the speed versus IPP (or time) values. It must be emphasized here that the speed estimates that we obtain are the radial or line-of-sight (LOS) values—deriving the velocity vector usually requires an interferometric and/or multistatic radar system, which we did not use for these observations. For event 1, the radial (LOS) entry speed of the system of fragments and the deceleration estimated from the linear fit are 12.5 km/s and 12.1 km/s^2, respectively.

III. Fine Parameter Estimation for Individual Fragments Using GA

The GA-based technique is designed to provide us with estimates of the parameters (amplitude, speed, and deceleration) of each fragment in the system. The GA algorithm starts with an initial population of random candidate parameters that are uniformly distributed over a small range around the initial Doppler estimates obtained from stage 1 of the technique. We define this range to be 0.5 km/s on either side of the radial speed estimate and 4 km/s^2 for deceleration estimate from stage 1. Then, through a process of *selection* (that refers to a process of choosing a proportion of the population based on fitness), *crossover* (or *recombination*, that refers to reproduction), and *mutation* (that refers to random changes in attributes of the offsprings to maintain diversity in population), successive generations possess better characteristics, which in our case refers to lower MSE. After some predetermined number of generations or when the average MSE of the population at a

TABLE I
MODELED PARAMETERS OF METEOR EVENT 1

IPP	Relative amplitude		Initial speed (km/s)		Deceleration (km/s^2)	
	Body 1	Body 2	Body 1	Body 2	Body 1	Body 2
1-5	1	0.5937	12.628	12.532	10.555	10.763
6-10	1	0.5937	12.519	12.428	10.062	10.445
11-15	1	0.5937	12.413	12.324	10.135	10.500
16-20	1	0.6493	12.304	12.219	9.5538	11.566
21-25	1	0.6996	12.192	12.103	8.9227	9.0333
26-30	1	0.7191	12.093	12.010	11.051	12.177
31-35	1	0.7707	11.812	11.734	9.7296	12.000

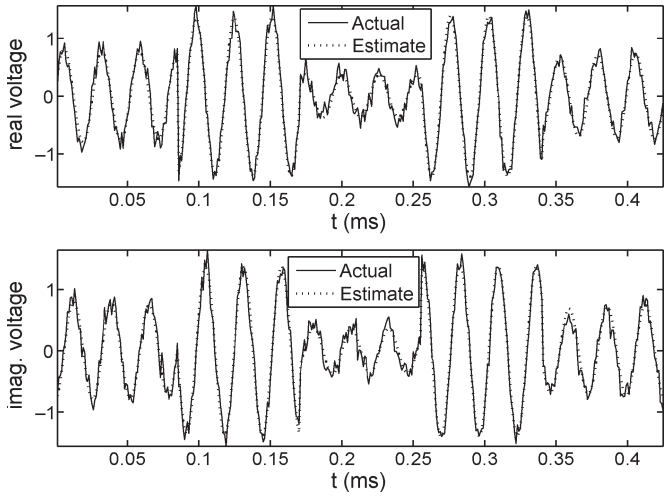

Fig. 3. Event 1 radar complex voltages and output of the model using parameters estimated by the GA technique for five IPPs stacked together.

particular generation reaches a predefined minimum, we stop the iterations and select from the final population the individual solution with the best characteristics as the final estimate.

Before moving on to the GA-based parameter estimation, a brief description of the physics of radar scattering from a point target is presented here. Consider that the ith meteoroid fragment is at range $R_i(t_0)$ at reference time t_0. Then, the complex baseband signal for the fragment is given by

$$x_i(t) = A_i \exp\left(\frac{i4\pi R_i(t)}{\lambda} t\right) \tag{1}$$

where $R_i(t)$, the range of the ith fragment at time t, is given by

$$R_i(t) = R_i(t_0) - \left(v_i - d_i \frac{t}{2}\right) t. \tag{2}$$

Here, v_i is the speed at time t_0, d_i is the deceleration, A_i is the amplitude of the ith fragment, and λ is the radar wavelength. The resultant signal, the baseband voltage, is the sum of the complex returns from all bodies. It must be pointed out here that although the description of meteor head-echo returns as a point target using (1) is well established in the literature for a single target [1], [6], [11], this is the first time that it is being applied to multiple fragments. Returning to the GA procedure, we begin with an initial population of random candidate parameters (A_i, v_i, d_i) from within a small range around the coarse estimates from stage 1 (as explained earlier). The synthetic complex baseband signal is then computed for each candidate parameter set by substituting these values in (1) and (2), and the MSE between the synthetic signal and the actual return signal is calculated for every candidate. A certain fraction of the candidate population having relatively high MSE is discarded, and a new population of candidates is generated through a process of selection, crossover, and mutation. This procedure is then repeated for a fixed number of iterations or until the minimum MSE of the population drops below a particular threshold.

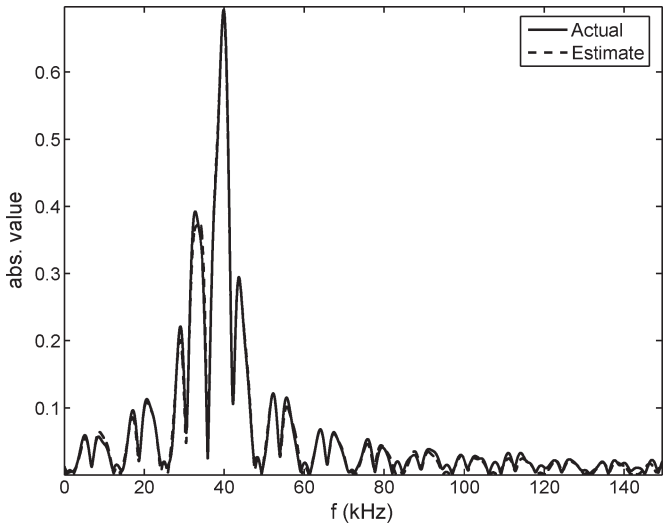

Fig. 4. FFT of actual signal and output of the model using parameters estimated by the GA technique for event 1.

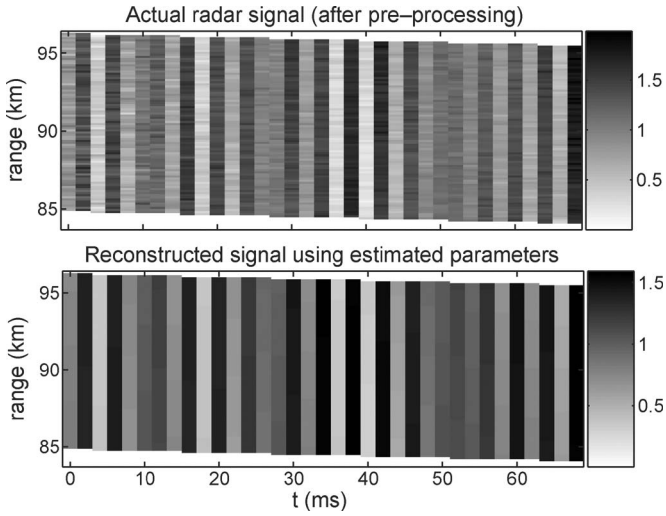

Fig. 5. RTI plot of the actual radar signal after preprocessing (upper panel) and reconstructed RTI plot using estimated parameters from our technique (lower panel) for event 1.

As part of our procedure, we stack (group sequentially) meteor signals from consecutive IPPs and try to find the set of model parameters that leads to the minimum MSE. The issue of how many IPPs to stack together for GA analysis needs some discussion. On the one hand, a longer time series leads to a better estimate of model parameters particularly if the number of parameters to be estimated is large, while on the other hand, the fact that the parameters of the meteoroid fragments change continuously as they travel through the atmosphere would indicate that considering a smaller data series would

TABLE II
MODELED PARAMETERS OF METEOR EVENT 2

IPP	Relative amplitude			Initial speed (km/s)			Deceleration (km/s^2)		
	Body 1	Body 2	Body 3	Body 1	Body 2	Body 3	Body 1	Body 2	Body 3
1-5	1	0.8453	0.6050	21.704	21.759	21.450	51.650	50.433	42.710
6-10	1	0.8163	0.4283	21.469	21.555	21.023	40.681	47.089	32.226
11-15	1	0.7224	0.2986	20.875	21.216	20.768	47.283	56.154	47.546
16-20	1	0.9021	0.5092	20.816	20.997	20.311	75.442	52.605	36.215
21-25	1	0.8890	0.5088	20.026	20.372	19.864	26.036	15.618	37.033
26-30	1	0.8922	0.5107	19.589	20.022	19.311	68.718	43.410	50.551

TABLE III
MODELED PARAMETERS OF METEOR EVENT 3

IPP	Relative amplitude		Initial speed (km/s)		Deceleration (km/s^2)	
	Body 1	Body 2	Body 1	Body 2	Body 1	Body 2
1-5	1	0.3516	27.491	27.476	6.4265	14.319
6-10	1	0.3389	27.403	27.357	6.1168	10.544
11-15	1	0.3869	27.341	27.276	9.4601	13.411
16-20	1	0.3999	27.230	27.199	6.6598	19.040
21-25	1	0.3804	27.146	27.052	7.8776	8.3988
26-30	1	0.3879	27.065	26.978	10.617	14.012

better capture the transient parameters of the bodies by our simple model. Our studies indicate that $N_{\mathrm{IPP}} = 5$ produces optimum results as far as estimating fragment parameters is concerned.

The next task is to determine the model order. Since the number of scattering fragments is not known in advance, we assume one meteoroid fragment to be present initially and then progressively increase the number of fragments assumed in the model to determine the model size at which the MSE value stops decreasing. For event 1, we determined that two fragments are present, and the individual parameters are listed in Table I. Only the first 35 IPPs yielded reliable estimates of the parameters and are included in the table. The closeness of the model generated using the estimated parameters and the actual radar signal is shown in Figs. 3 and 4 where we show the time series and the absolute value of the FFT of the actual radar signal and the estimated model. In addition, by examining the initial speeds and the decelerations, we can project back in time to determine when the speeds of the two fragments are equal, which would indicate the time when fragmentation occurred. For event 1, we determined that fragmentation occurred 460 ms before the fragments entered the radar beam, assuming that their parameters remained constant.

Furthermore, by using the estimated values of radial speed and deceleration, we can calculate how rapidly the two fragments are separating from each other. The estimated parameters indicate that the separation between the fragments increases by about 6 m over the duration of 70 ms for which parameter estimates are available. Finally, in Fig. 5, we show the reconstructed range–time–intensity (RTI) plot for the portion of the event for which we estimate the parameters. This seems to match the RTI plot of the actual radar signal, which of course also includes background noise.

Event 2 appears to have a more complicated structure compared to event 1. A close examination of the RTI plot reveals rapid fading of the signal within a particular pulse return (over 90 μs), thereby indicating the possibility of the presence of more than two fragments. We applied the parameter estimation technique to this event with successively increasing model order and noted the minimum MSE achieved in each case. We find that as we increase the model order from two to three bodies, the minimum MSE decreases, but it remains about the same when going from three to four. From this, we conclude that a third-order model is sufficient to represent the event. Following a method similar to that for event 1, we derive the estimated parameters for this event that are listed in Table II. Event 3 is similar to event 1, and the results obtained using the GA analysis are presented in Table III. In this case, 30 central IPPs were utilized for parameter estimation. The SNR curve for this event [Fig. 1(c)] exhibits large variation in frequency. To explain this phenomenon, we note that a simple extension of (1) shows that the amplitude of the resultant baseband voltage is a sinusoid of frequency $(R_1(t) - R_2(t))/\lambda$. Since radial separation of the fragments $(R_1(t) - R_2(t))$ varies with time, so also does the frequency of their amplitude oscillations.

IV. CONCLUSION

In this letter, we have used a simple but well-established mathematical model to represent the radar signal observed due to fragmenting meteoroids that involves three parameters per fragment and have developed a two-stage procedure to estimate those parameters. In the first stage, the approximate speed of the system of bodies is estimated using the FFT. This estimate is used to define the parameter search space for the second stage which is a GA-based parameter estimator. This stage converges to the values of the relative mass, radial velocity, and deceleration within the search space that minimize the MSE between the actual return signal and the synthetic signal generated using the candidate parameters. Application of this technique to fragmentation events yielded parameter estimates that were physically consistent and resulted in very small error between the synthetically generated and the real radar signals.

While this letter has been principally directed toward extending the use of the basic model developed for a single point target to the radar return from two or more related meteoroid

fragments via GA processing, the importance of this effort to the radio science results must be emphasized. In particular, the depth of modulation in all three examples cited in this letter underscores that each fragment has a well-defined scattering center, thus supporting the use of the point (much less than a wavelength) target model developed in our earlier work. That such apparently diverse events such as one that displays signal fading within the 90-μs pulse (which we show is due to the presence of three fragments) and another that shows complex modulation (which is shown to have a simple interpretation as two fragments) are convincingly described by our technique clearly supports its validity. These important radio science outcomes of the GA technique will be the subject of a full paper.

REFERENCES

[1] J. D. Mathews, "Radio science issues surrounding HF/VHF/UHF radar meteor studies," *J. Atmos. Sol.-Terr. Phys.*, vol. 66, no. 3, pp. 285–299, Feb./Mar. 2004.

[2] J. D. Mathews, D. D. Meisel, K. P. Hunter, V. S. Getman, and Q. Zhou, "Very high resolution studies of micrometeors using the Arecibo 430 MHz radar," *Icarus*, vol. 126, no. 1, pp. 157–169, Mar. 1997.

[3] A. Pellinen-Wannberg, "Meteor head echoes: Observations and models," *Annales Geophys.*, vol. 203, no. 1, pp. 201–205, Jan. 2005.

[4] J. Jones, W. Jones, and I. Halliday, "The head echo problem—A solution at last?" in *Proc. Meteoroids Conf.*, Tatranska Lomnica, Slovakia, Aug. 17–21, 1999, pp. 29–36.

[5] S. Close, M. Oppenheim, S. Hunt, and A. Coster, "A technique for calculating meteor plasma density and meteoroid mass from radar head echo scattering," *Icarus*, vol. 168, no. 1, pp. 43–52, Mar. 2004.

[6] S. J. Briczinski, C.-H. Wen, J. D. Mathews, J. F. Doherty, and Q.-N. Zhou, "Robust voltage techniques for meteor Doppler speed determination," *IEEE Trans. Geosci. Remote Sens.*, vol. 44, no. 12, pp. 3490–3496, Dec. 2006.

[7] J. D. Mathews, J. F. Doherty, C.-H. Wen, S. J. Briczinski, D. Janches, and D. D. Meisel, "An update on UHF radar meteor observations and associated signal processing techniques at Arecibo observatory," *J. Atmos. Sol.-Terr. Phys.*, vol. 65, no. 10, pp. 1139–1149, Jul. 2003.

[8] C.-H. Wen, S. J. Briczinski, D. J. Livneh, J. F. Doherty, and J. D. Mathews, "Pulse-level interference and meteor processing of Arecibo ISR data," *J. Atmos. Sol.-Terr. Phys.*, vol. 69, no. 9, pp. 973–980, Jul. 2007.

[9] C.-H. Wen, J. F. Doherty, and J. D. Mathews, "Time-frequency radar processing for meteor detection," *IEEE Trans. Geosci. Remote Sens.*, vol. 42, no. 3, pp. 501–510, Mar. 2004.

[10] W. G. Elford and L. Campbell, "Effects of meteoroid fragmentation on radar observations of meteor trails," in *Proc. Meteoroids Conf.*, Kiruna, Sweden, Aug. 6–10, 2001, pp. 419–423.

[11] J. Kero, C. Szasz, A. Pellinen-Wannenberg, A. Westman, and D. D. Meisel, "Three-dimensional radar observation of a submillimeter meteoroid fragmentation," *Geophys. Res. Lett.*, vol. 35, no. 4, pp. 1–5, Feb. 2008.

[12] S. Close, T. Hamlin, M. Oppenheim, L. Cox, and P. Colestock, "Dependence of radar signal strength on frequency and aspect angle of nonspecular meteor trails," *J. Geophys. Res.*, vol. 113, no. A6, pp. 1–8, Jun. 2008.

[13] A. Konak, D. W. Coit, and A. E. Smith, "Multi-object optimization using genetic algorithms: A tutorial," *Reliab. Eng. Syst. Saf.*, vol. 91, no. 9, pp. 992–1007, Sep. 2006.

[14] D. Whitley, "A genetic algorithm tutorial," *Stat. Comput.*, vol. 4, no. 2, pp. 65–85, Jun. 1994.